3 Theory

This chapter presents the theoretical background for interpretation of solid-state NMR spectra in terms of the quadrupole coupling and CSA interactions. Particular focus is put on the interpretation of SC NMR spectra. This theory is incorporated into the ASICS software package for simulation of SC NMR spectra and described in chapter 4. Finally, a short introduction to simulation of powder spectra (MAS or static) in terms of the same interactions is also given. Such simulations are performed by the software package STARS (Spectrum Analysis of Rotating Solids) developed by Henrik Bildsøe (*46*, *74*) and incorporated in Varian's solid-state NMR software package.

3.1 The Hamiltonian

The Hamiltonian for a nucleus in an external magnetic field and exposed to an rf irradiation is given by

$$\mathcal{H} = \mathcal{H}_{\mathrm{Z}} + \mathcal{H}_{\mathrm{Q}} + \mathcal{H}_{\sigma} + \mathcal{H}_{\mathrm{D}} + \mathcal{H}_{\mathrm{J}} + \mathcal{H}_{\mathrm{rf}} \tag{3.1}$$

where $\mathcal{H}_{\mathrm{Z}}$ represents the Zeeman interaction, $\mathcal{H}_{\mathrm{Q}}$ the quadrupole coupling interaction, $\mathcal{H}_{\sigma}$ the CSA interaction, $\mathcal{H}_{\mathrm{D}}$ the dipole coupling (through space) interaction, $\mathcal{H}_{\mathrm{J}}$ the J coupling (through bond) interaction, and $\mathcal{H}_{\mathrm{rf}}$ is the rf irradiation Hamiltonian. In all studies presented in this report the dipolar and J coupling interactions will be negligible – either by nature or, in some cases, due to broad-band proton decoupling. The rf Hamiltonian is mainly of interest if we consider fancy pulse sequences or non-ideal excitation. In this thesis I shall show no simulations that

requires use of the rf Hamiltonian and, therefore, it will be omitted in the remainig of this chapter. Thus, the Hamiltonian of interest is given by

$$\mathcal{H} = \mathcal{H}_{\mathrm{Z}} + \mathcal{H}_{\mathrm{Q}} + \mathcal{H}_{\sigma}. \tag{3.2}$$

According to Mehring (*75*) these terms may be expressed as[1]

$$\mathcal{H}_{\mathrm{Z}} = -\gamma \mathrm{I}^{\dagger} \cdot \mathbf{1} \cdot \mathrm{B}_0 = \omega_0 I_z \tag{3.3}$$

$$\mathcal{H}_{\mathrm{Q}} = \mathrm{I}^{\dagger} \cdot \mathbf{Q} \cdot \mathrm{I} \tag{3.4}$$

$$\mathcal{H}_{\sigma} = \gamma \mathrm{I}^{\dagger} \cdot \boldsymbol{\sigma} \cdot \mathrm{B}_0 \tag{3.5}$$

where B_0 is the external magnetic field which has an orientation along the z axis, ω_0 is the Larmor frequency for the nucleus with the gyromagnetic ratio γ, $\mathbf{Q}$ is the quadrupole coupling tensor ($\mathbf{Q} = eQ/\{2I(2I-1)\}\mathbf{V}$ where $\mathbf{V}$ is the electric field gradient (EFG) tensor and I is the nuclear spin), and $\boldsymbol{\sigma}$ is the chemical shielding tensor.[2]

It is often a good idea to describe the quadrupole coupling and CSA Hamiltonians (eqs. 3.4 and 3.5) by irreducible tensors (*76*) rather than by the cartesian tensors used in eqs. 3.4 and 3.5. In the irreducible tensor formalism the quadrupole coupling and CSA Hamiltonians become

$$\mathcal{H}_{\lambda} = \lambda^{\mathrm{L}}_{00} T^{\lambda}_{00} + \sum_{m=-2}^{2} (-1)^m \lambda^{\mathrm{L}}_{2-m} T^{\lambda}_{2m}. \tag{3.6}$$

$\lambda^{\mathrm{L}}_{jm}$ represent the j'th rank irreducible spatial tensor elements of interaction λ (Q or σ) in the laboratory frame (L) and are listed in table 3.1. Table 3.2 summarizes

[1] *Nomenclature:* In this Thesis matrices and tensors will be in bold and sans serif ($\mathbf{A}$), vectors are upright (A), and tensor/matrix elements are in italic with their indices as subscripts ($A_{\alpha\beta}$).

[2] The tensors in eqs. 3.4 and 3.5 are not expressed in a specific frame. In the following, the frame in which the tensors/tensor elements are expressed will be indicated by a superscript, e.g., $\mathbf{Q}^{\mathrm{L}}$ for the quadrupole coupling tensor expressed in the laboratory (L) frame. However, the indication of the frame will be omitted for principal axis frames, e.g., $\sigma^{\mathrm{P}}_{xx} \equiv \sigma_{xx}$.

Table 3.1: Definition of irreducible tensor elements of rank 0, 1, and 2 for a symmetric cartesian tensor.

m	λ_{00}	λ_{1m}	λ_{2m}
0	$-1/\sqrt{3}\mathrm{Tr}(\boldsymbol{\lambda})$	0	$1/\sqrt{6}(3\lambda_{zz} - \mathrm{Tr}(\boldsymbol{\lambda}))$
± 1		0	$\mp\lambda_{xz} - i\lambda_{yz}$
± 2			$1/2(\lambda_{xx} - \lambda_{yy}) \pm i\lambda_{xy}$

Table 3.2: Irreducible spin tensor elements, T^{λ}_{jm}, for the CSA and quadrupole coupling interactions.

	σ	Q
T^{λ}_{00}	$-1/\sqrt{3}I_z\omega_0$	0
T^{λ}_{20}	$\sqrt{2/3}I_z\omega_0$	$1/\sqrt{6}\,(3I_z^2 - I(I+1))$
$T_{2\pm1}$	$\mp 1/2 I_{\pm}\omega_0$	$\mp 1/2\,(I_zI_{\pm} + I_{\pm}I_z)$
$T^{\lambda}_{2\pm2}$	0	$1/2 I_{\pm}I_{\pm}$

the spin tensor elements T^{λ}_{jm}.[3] It is noted that the element Q_{00} equals zero because the quadrupole coupling tensor is traceless.

The magnitudes of quadrupole coupling and chemical shielding interaction are given by the quadrupole coupling parameters

$$C_{\mathrm{Q}} = \frac{eQ}{h}V_{zz} \qquad \eta_{\mathrm{Q}} = \frac{V_{yy} - V_{xx}}{V_{zz}} \tag{3.7}$$

and the chemical shielding parameters

$$\delta_{\mathrm{iso}} = \sigma_{\mathrm{ref}} - \frac{1}{3}\mathrm{Tr}(\boldsymbol{\sigma}) \qquad \delta_{\sigma} = \sigma_{zz} - \frac{1}{3}\mathrm{Tr}(\boldsymbol{\sigma}) \qquad \eta_{\sigma} = \frac{\sigma_{yy} - \sigma_{xx}}{\delta_{\sigma}} \tag{3.8}$$

[3]Equation 3.6 contains only irreducible tensor elements of rank 0 and 2. In principle it should also include a summation of the tensor elements of rank 1. However, the first rank tensor elements only contain information about the asymmetry of the cartesian tensor and thus, they equal zero for a symmetric tensor. The quadrupole coupling tensor is symmetric by nature, and the CSA tensor is usually symmetrized (Any tensor may be decomposed to a symmetric and an antisymmetric part according to $\mathbf{A} = \mathbf{A}_{\mathrm{sym}} + \mathbf{A}_{\mathrm{anti}}$ where $\mathbf{A}_{\mathrm{sym}} = 1/2(\mathbf{A} + \mathbf{A}^T)$ and $\mathbf{A}_{\mathrm{anti}} = 1/2(\mathbf{A} - \mathbf{A}^T)$) why eq. 3.6 is valid in our case.

where σ_{ref} is the shielding of a reference compound (e.g., TMS for ^{1}H).[4]

Indeed it is possible to determine the eigenvalues for the Hamiltonian by diagonalization if the spin operators are written in matrix form (*75*), and in the presence of very large interactions this is the correct approach. However, the diagonalization procedure is computationally rather time consuming and thus, it is of interest to avoid the diagonalization.

3.1.1 "Removal" of the Zeeman Interaction

For the NMR spectroscopist the Zeeman interaction is of no interest because it contains no information about the particular compound under investigation. Moreover, the Zeeman interaction is eliminated from the experimental free-induction decay (FID) by a demodulation of the FID that "removes" the carrier/Larmor frequency and thereby the Zeeman interaction.

The general approach to a theoretical "removal" of the Zeeman interaction involves a coordinate transformation in the spin space.[5] The description of the spin part of the Hamiltonian in eq. 3.2 is transferred from the laboratory frame to a frame that rotates about the z/B_0-field axis with the Larmor frequency - the socalled Zeeman-interaction representation which is denoted by a tilde. This eliminates the

[4] There are numerous definitions of the chemical shielding parameters in the litterature. Most of the confusion is caused by the sign of the shielding parameters. The definition used here implies that the σ (shielding) scale for the shielding elements $\sigma_{\alpha\beta}$ has its origin at the shielding for the bare nucleus. On the other hand, the δ (shift) scale, which is normally used, has the opposite direction of the σ scale and is defined by $\delta = \sigma_{\text{ref}} - \sigma$.

[5] The spin-state of the system may be described by the density operator ρ ($= \overline{|\psi\rangle\langle\psi|}$, where the wave-function is expressed as a linear combination of the Zeeman states ($|m\rangle$) as $|\psi\rangle = \sum_m c_m|m\rangle$). The evolution of the density operator is given by the Liouville von Neumann equation, $d\rho/dt = -i[\mathcal{H}, \rho]$, and the Hamiltonian is given by $\mathcal{H} = \mathcal{H}_{\mathrm{Z}} + \mathcal{H}_\lambda$. The trick is to define a new density operator, $\widetilde{\rho}$, given by $\widetilde{\rho} = e^{i\mathcal{H}_{\mathrm{Z}}t} \cdot \rho \cdot e^{-i\mathcal{H}_{\mathrm{Z}}t}$. The time-derivative of this density operator is $d\widetilde{\rho}/dt = d/dt(e^{i\mathcal{H}_{\mathrm{Z}}t}) \cdot \rho \cdot e^{-i\mathcal{H}_{\mathrm{Z}}t} + e^{i\mathcal{H}_{\mathrm{Z}}t} \cdot d\rho/dt \cdot e^{-i\mathcal{H}_{\mathrm{Z}}t} + e^{i\mathcal{H}_{\mathrm{Z}}t} \cdot \rho \cdot d/dt(e^{-i\mathcal{H}_{\mathrm{Z}}t}) = e^{i\mathcal{H}_{\mathrm{Z}}t} \cdot d\rho/dt \cdot e^{-i\mathcal{H}_{\mathrm{Z}}t} + i[\mathcal{H}_{\mathrm{Z}}, \widetilde{\rho}]$ (a). By inserting the Liouville von Neumann equation into the first term it becomes $e^{i\mathcal{H}_{\mathrm{Z}}t} \cdot d\rho/dt \cdot e^{-i\mathcal{H}_{\mathrm{Z}}t} = -ie^{i\mathcal{H}_{\mathrm{Z}}t}[\mathcal{H}, \rho]e^{-i\mathcal{H}_{\mathrm{Z}}t} = -i[e^{i\mathcal{H}_{\mathrm{Z}}t}(\mathcal{H}_{\mathrm{Z}} + \mathcal{H}_\lambda)e^{-i\mathcal{H}_{\mathrm{Z}}t}, \widetilde{\rho}]$. The Zeeman term of this commutator cancels the last term in eq. (a) and thus, the equation of motion for $\widetilde{\rho}$ is given by $d\widetilde{\rho}/dt = -i[\widetilde{\mathcal{H}}_\lambda, \widetilde{\rho}]$, where $\widetilde{\mathcal{H}}_\lambda = e^{i\mathcal{H}_{\mathrm{Z}}t}\mathcal{H}_\lambda e^{-i\mathcal{H}_{\mathrm{Z}}t}$.

Zeeman interaction from the Hamiltonian which becomes

$$\widetilde{\mathcal{H}} = \widetilde{\mathcal{H}}_{\mathrm{Q}} + \widetilde{\mathcal{H}}_{\sigma} + \widetilde{\mathcal{H}}_{\mathrm{rf}} \tag{3.9}$$

and introduces a time modulation of the quadrupole coupling and CSA terms according to

$$\begin{aligned} \widetilde{\mathcal{H}}_{\lambda} &= \lambda^{\mathrm{L}}_{00} e^{i\omega_0 t I_z} T^{\lambda}_{00} e^{-i\omega_0 t I_z} + \sum_{m=-2}^{2} (-1)^m \lambda^{\mathrm{L}}_{2-m} e^{i\omega_0 t I_z} T^{\lambda}_{2m} e^{-i\omega_0 t I_z} \\ &= \lambda^{\mathrm{L}}_{00} T^{\lambda}_{00} + \sum_{m=-2}^{2} (-1)^m \lambda^{\mathrm{L}}_{2-m} T^{\lambda}_{2m} e^{-im\omega_0 t} = \widetilde{\mathcal{H}}_{\lambda}(t). \end{aligned} \tag{3.10}$$

3.1.2 Average Hamiltonian Theory

Magnus (*77*) developped a general tool to average a periodic time dependence of an operator, a tool that has been introduced in solid-state NMR by Haeberlen and Waugh (*78*). The periodic of the Hamiltonian in eq. 3.9 (with the period $\tau_0 = 2\pi/\omega_0$) may be replaced by its average Hamiltonian

$$\overline{\widetilde{\mathcal{H}}} = \frac{1}{\tau_0}\int_0^{\tau_0} \widetilde{\mathcal{H}}(t)dt + \frac{-i}{2\tau_0}\int_0^{\tau_0} dt \int_0^t \left[\widetilde{\mathcal{H}}(t), \widetilde{\mathcal{H}}(t')\right] dt' + \ldots \tag{3.11}$$

$$= \overline{\widetilde{\mathcal{H}}}^{(1)} + \overline{\widetilde{\mathcal{H}}}^{(2)} + \ldots \tag{3.12}$$

where $\overline{\widetilde{\mathcal{H}}}^{(n)}$ represents the n'th-order term of the average Hamiltonian.[6] The Zeeman interaction is normally much larger than the other interactions and, therefore, it is normally adequate to include the first two terms of the average Hamiltonian since the n'th order term is proportional to $(\mathcal{H}_{\lambda})^n/\omega_0^{n-1}$. This approximation is normally referred to as the high-field approximation. The first-order term is a sum of two terms from the CSA and quadrupole coupling interactions ($\overline{\widetilde{\mathcal{H}}}^{(1)} = \overline{\widetilde{\mathcal{H}}}^{(1)}_{\sigma} + \overline{\widetilde{\mathcal{H}}}^{(1)}_{\mathrm{Q}}$) while a mixing term arises between the interactions in the second-order term ($\overline{\widetilde{\mathcal{H}}}^{(2)} =$

[6] According to Magnus (*77*) the first term in eq. 3.12 is the 0'th order term, as also generally used in NMR (*78*). However, the numbering of the quadrupolar terms is traditionally that of eq. 3.12.

$\overline{\overline{\mathcal{H}}}_{\sigma}^{(2)} + \overline{\overline{\mathcal{H}}}_{\mathrm{Q}}^{(2)} + \overline{\overline{\mathcal{H}}}_{\mathrm{Q},\sigma}^{(2)}$), although only the second-order quadrupolar term is important while the remaining terms are too small to observe.

In the high-field regime ($\mathcal{H}_{\mathrm{Z}} \gg \mathcal{H}_{\lambda}$) we may use the Zeeman Eigenfunctions ($|m\rangle$) as Eigenbasis for the average Hamiltonian. Moreover, it is assumed that there is no mixing between the Zeeman Eigenfunctions which implies that only diagonal elements of the average Hamiltonian should be included, i.e., only elements $\langle m|\,\overline{\overline{\mathcal{H}}}\,|m'\rangle$ with $m = m'$ are included.[7]

The relevant terms of the average Hamiltonian in the high-field and secular approximations are given by

$$\overline{\overline{\mathcal{H}}}_{\sigma}^{(1)} = \sigma_{00}^{\mathrm{L}} T_{00}^{\sigma} + \sigma_{20}^{\mathrm{L}} T_{20}^{\sigma} = \frac{\omega_0}{\sqrt{3}} \left(-\sigma_{00}^{\mathrm{L}} + \sqrt{2}\sigma_{20}^{\mathrm{L}}\right) I_z \tag{3.13}$$

$$\overline{\overline{\mathcal{H}}}_{\mathrm{Q}}^{(1)} = Q_{20}^{\mathrm{L}} T_{20}^{\mathrm{Q}} = \frac{1}{\sqrt{6}} Q_{20}^{\mathrm{L}} \left\{3I_z^2 - I(I+1)\right\} \tag{3.14}$$

$$\begin{aligned}\overline{\overline{\mathcal{H}}}_{\mathrm{Q}}^{(2)} &= \frac{1}{2\omega_0}\left(Q_{2-2}^{\mathrm{L}} Q_{22}^{\mathrm{L}} \left[T_{22}^{\mathrm{Q}}, T_{2-2}^{\mathrm{Q}}\right] + 2Q_{2-1}^{\mathrm{L}} Q_{21}^{\mathrm{L}} \left[T_{21}^{\mathrm{Q}}, T_{2-1}^{\mathrm{Q}}\right]\right) \\ &= \frac{1}{2\omega_0}\left(Q_{2-2}^{\mathrm{L}} Q_{22}^{\mathrm{L}} \left\{2I(I+1) - 2I_z^2 - 1\right\} I_z \right. \\ &\qquad \left. + Q_{2-1}^{\mathrm{L}} Q_{21}^{\mathrm{L}} \left\{4I(I+1) - 8I_z^2 - 1\right\} I_z\right)\end{aligned} \tag{3.15}$$

3.1.3 Coordinate Transformations

The principal elements of the spatial tensors are given in eqs. 3.7 and 3.8 but the Hamiltonians (eqs. 3.13 - 3.15) are expressed in the laboratory frame. Coordinate transformations may be carried out in either the irreducible or cartesian tensor formalism. A transformation from frame F1 to frame F2 in the irreducible tensor basis corresponds to the matrix multiplication

[7] The validity of this socalled secular approximation has been investigated in our ^{71}Ga and ^{69}Ga SC NMR study of β-Ga_2O_3 (*79*). The ^{69}Ga spectra for the tetrahedral Ga site were interpreted by diagonalization of the Hamiltonian in eq. 3.2 in the $|m\rangle$ basis which provides the possiblilty to investigate the mixing between the different Zeeman Eigenfunctions. The result showed that for the ^{69}Ga quadrupole coupling constant of $C_{\mathrm{Q}} \approx 18$ MHz ($C_{\mathrm{Q}}/\{2I(2I-1)\} \approx 3$ MHz and with a Larmor frequency of $\nu_0 = 96$ MHz there is less than a 2% mixing between the Zeeman Eigenfunctions.

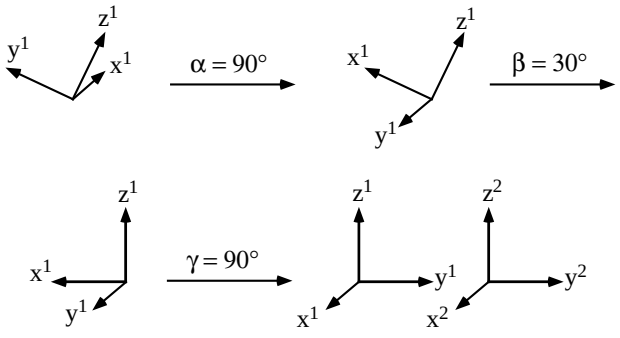

Figure 3.1: Illustration of the coordinate transformation from F1 to F2 by three individual rotations. This particular transformation corresponds the the Euler angles $(\alpha, \beta, \gamma) = (90°, 30°, 90°)$.

$$\lambda_{lm}^{\mathrm{F2}} = \sum_{m'=-l}^{l} \lambda_{lm'}^{\mathrm{F1}} \mathfrak{D}_{m'm}^{(l)}(\alpha, \beta, \gamma). \tag{3.16}$$

The Euler angles α, β, and γ indicate the rotation angle for the rotation about the z^1 (α), the new y^1 (β), and the new z^1 (γ) axis as illustrated in fig. 3.1 (*75*). $\mathfrak{D}_{m'm}^{(l)}$ represent the (m', m)'th element of the l'th order Wigner-rotation matrix (*76*).

In the cartesian representation the coordinate transformation is given by

$$\boldsymbol{\lambda}^{\mathrm{F2}} = \mathbf{R}^{\mathrm{F1F2}}(\alpha, \beta, \gamma) \cdot \boldsymbol{\lambda}^{\mathrm{F1}} \cdot (\mathbf{R}^{\mathrm{F1F2}})^T(\alpha, \beta, \gamma), \tag{3.17}$$

i.e., $\lambda_{\alpha\beta}^{\mathrm{F2}} = \sum_{\gamma,\delta=x,y,z} (R^{\mathrm{F1F2}})_{\alpha\gamma} (R^{\mathrm{F1F2}})_{\beta\delta} \lambda_{\gamma\delta}^{\mathrm{F1}}$, and with the rotation matrix

$$\mathbf{R}^{\mathrm{F1F2}}(\alpha, \beta, \gamma) = \begin{pmatrix} \cos\alpha\cos\beta\cos\gamma - \sin\alpha\sin\gamma & \sin\alpha\cos\beta\cos\gamma + \cos\alpha\sin\gamma & -\sin\beta\cos\gamma \\ -\cos\alpha\cos\beta\sin\gamma - \sin\alpha\cos\gamma & -\sin\alpha\cos\beta\sin\gamma + \cos\alpha\cos\gamma & \cos\beta\cos\gamma \\ \cos\alpha\sin\beta & \sin\alpha\sin\beta & \cos\gamma \end{pmatrix} \tag{3.18}$$

being in accordance with Spiess (*80*).

3.2 Simulation of Single-Crystal NMR Spectra

For simulation of SC NMR spectra it is useful to express the Hamiltonians in the cartesian basis as

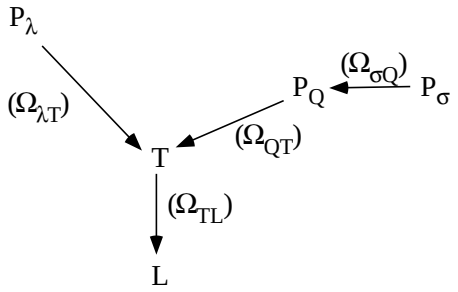

Figure 3.2: Coordinate transformations used to calculate the $\boldsymbol{\lambda}^{\mathrm{L}}$ tensor from $\boldsymbol{\lambda}^{\mathrm{P}}$. The route to the left applies in the presence of only one interaction while the route to the right is used for the combined effect of quadrupole coupling and CSA.

$$\overline{\widetilde{\mathcal{H}}}_{\sigma}^{(1)} = \nu_0 \sigma_{zz}^{\mathrm{L}} I_z \tag{3.19}$$

$$\overline{\widetilde{\mathcal{H}}}_{\mathrm{Q}}^{(1)} = 3Q_{zz}^{\mathrm{L}} \left\{ 3I_z^2 - I(I+1) \right\} \tag{3.20}$$

$$\begin{aligned} \overline{\widetilde{\mathcal{H}}}_{\mathrm{Q}}^{(2)} = \frac{1}{2\nu_0} \Big\{ & \left[\left(Q_{xy}^{\mathrm{L}} \right)^2 + \frac{1}{4} \left(Q_{xx}^{\mathrm{L}} - Q_{yy}^{\mathrm{L}} \right)^2 \right] \left\{ 2I(I+1) - 2I_z^2 - 1 \right\} I_z \\ & - \left[\left(Q_{xz}^{\mathrm{L}} \right)^2 + \left(Q_{yz}^{\mathrm{L}} \right)^2 \right] \left\{ 4I(I+1) - 8I_z^2 - 1 \right\} I_z \Big\} \end{aligned} \tag{3.21}$$

by use of the expressions in table 3.1, and now in Hz instead of rad/s. The matrix elements of $\boldsymbol{\lambda}^{\mathrm{L}}$ are calculated from the principal elements given in eqs. 3.7 and 3.8 by the coordinate transformations shown in Fig. 3.2. In the presence of only one interaction the route is $\mathrm{P}_\lambda \rightarrow \mathrm{T} \rightarrow \mathrm{L}$ where the Euler angles $\Omega_{\lambda\mathrm{T}} = (\alpha_\lambda, \beta_\lambda, \gamma_\lambda)$ define the first coordinate transformation. If both the quadrupole coupling and CSA interactions are present the route is $\mathrm{P}_\sigma \rightarrow \mathrm{P}_\mathrm{Q} \rightarrow \mathrm{T} \rightarrow \mathrm{L}$. In this case the relative orientation of the P_σ and P_Q frames is described by the Euler angles $\Omega_{\sigma\mathrm{Q}} = (\psi, \chi, \xi)$. The coordinate transformation from the tenon frame to the laboratory frame depends on the rotation axis (α) and the rotation angle for the goniometer (θ).

The resonance frequencies for the secular Hamiltonian are given by the energy splitting between the Zeeman levels

$$\nu_m = \langle m | \overline{\widetilde{\mathcal{H}}} | m \rangle - \langle m-1 | \overline{\widetilde{\mathcal{H}}} | m-1 \rangle , \tag{3.22}$$

and may be separated into contributions from the individual terms of the Hamiltonian according to $\nu_{m,\alpha}(\theta) = \nu_{m,\alpha}^{\sigma,1}(\theta) + \nu_{m,\alpha}^{\mathrm{Q},1}(\theta) + \nu_{m,\alpha}^{\mathrm{Q},2}(\theta)$ where the dependences of

θ and α have been included.

It is convenient to express the resonance frequency in terms of the $\lambda^{\mathrm{T}}_{\alpha\beta}$ elements because some relatively simple expressions are then obtained as shown in the following sections. Furthermore, these elements are calculated from the principal elements by the matrix multiplications

$$\lambda^{\mathrm{T}}_{ij} = \sum_{k=x,y,z} (R^{\mathrm{PT}})_{ik} (R^{\mathrm{PT}})_{jk} \lambda^{\mathrm{P}}_{kk} \tag{3.23}$$

$$\sigma^{\mathrm{T}}_{ij} = \sum_{k,l=x,y,z} (R^{\mathrm{QT}})_{ik} (R^{\mathrm{QT}})_{jl} \left(\sum_{m=x,y,z} (R^{\mathrm{PQ}})_{km} (R^{\mathrm{PQ}})_{lm} \sigma^{\mathrm{P}}_{mm} \right). \tag{3.24}$$

Equation 3.23 is used when only one interaction is present while eq. 3.24 is used to calculate the CSA tensor in the tenon frame when both the CSA and quadrupole coupling interactions are present.

3.2.1 The Three-Axis Goniometer

The coordinate transformation from T to L is obviously different for the three axes rotation and depends on the rotation angle θ for the stepwise rotation of the goniometer. For the three-axis goniometer described in section 2.1 the T $\rightarrow$ L coordinate transformation is described by the rotation matrices

$$\mathbf{R}_x(\theta) = \begin{pmatrix} 1 & 0 & 0 \\ 0 & \cos\theta & \sin\theta \\ 0 & -\sin\theta & \cos\theta \end{pmatrix} \tag{3.25}$$

$$\mathbf{R}_y(\theta) = \begin{pmatrix} 0 & -1 & 0 \\ \cos\theta & 0 & \sin\theta \\ -\sin\theta & 0 & \cos\theta \end{pmatrix} \tag{3.26}$$

$$\mathbf{R}_z(\theta) = \begin{pmatrix} 0 & 0 & 1 \\ \sin\theta & -\cos\theta & 0 \\ \cos\theta & \sin\theta & 0 \end{pmatrix}. \tag{3.27}$$

Table 3.3: Coefficients, $M^{\lambda,n}_{m,\alpha}$, for eqs. 3.28 and 3.29 expressed in terms of the $\lambda^{\mathrm{T}}_{\alpha\beta}$ tensor elements. The $M^{\mathrm{Q},2}_{m,\alpha}$ elements are only listed for the central transition ($m = 1/2$). The nomenclature used is $\Gamma_\sigma = -\nu_0$, $\Gamma_{\mathrm{Q}} = 3(m - 1/2)$, and for the central transition $\Lambda_{\mathrm{Q}} = (3 - 4I[I+1])/16\nu_0$. $(\alpha, \beta, \gamma, \mu) = (x, y, z, 1)$, $(y, x, z, 1)$, or $(z, x, y, -1)$.

$A^{\lambda,1}_{m,\alpha}$	$\Gamma_\lambda/2\left(\lambda^{\mathrm{T}}_{\gamma\gamma} + \lambda^{\mathrm{T}}_{\beta\beta}\right)$
$B^{\lambda,1}_{m,\alpha}$	$\Gamma_\lambda\mu/2\left(\lambda^{\mathrm{T}}_{\gamma\gamma} - \lambda^{\mathrm{T}}_{\beta\beta}\right)$
$C^{\lambda,n}_{m,\alpha}$	$\Gamma_\lambda\mu\lambda^{\mathrm{T}}_{\beta\gamma}$
$A^{\mathrm{Q},2}_{\frac{1}{2},\alpha}$	$\Lambda_{\mathrm{Q}}/8\left[8Q^{\mathrm{T}}_{\alpha\alpha}\left(Q^{\mathrm{T}}_{\beta\beta} + Q^{\mathrm{T}}_{\gamma\gamma} - Q^{\mathrm{T}}_{\alpha\alpha}\right) + 16\left((Q^{\mathrm{T}}_{\alpha\beta})^2 + (Q^{\mathrm{T}}_{\alpha\gamma})^2\right)\right.$ $\left. +5\left((Q^{\mathrm{T}}_{\beta\beta})^2 + (Q^{\mathrm{T}}_{\gamma\gamma})^2\right) + 28(Q^{\mathrm{T}}_{\beta\gamma})^2 - 18Q^{\mathrm{T}}_{\beta\beta}Q^{\mathrm{T}}_{\gamma\gamma}\right]$
$B^{\mathrm{Q},2}_{\frac{1}{2},\alpha}$	$\Lambda_{\mathrm{Q}}\mu/2\left[2Q^{\mathrm{T}}_{\alpha\alpha}\left(Q^{\mathrm{T}}_{\beta\beta} - Q^{\mathrm{T}}_{\gamma\gamma}\right) - 12\left((Q^{\mathrm{T}}_{\alpha\beta})^2 - (Q^{\mathrm{T}}_{\alpha\gamma})^2\right) - (Q^{\mathrm{T}}_{\beta\beta})^2 + (Q^{\mathrm{T}}_{\gamma\gamma})^2\right]$
$C^{\mathrm{Q},2}_{\frac{1}{2},\alpha}$	$-\Lambda_{\mathrm{Q}}\mu\left[-2Q^{\mathrm{T}}_{\alpha\alpha}Q^{\mathrm{T}}_{\beta\gamma} + 12Q^{\mathrm{T}}_{\alpha\beta}Q^{\mathrm{T}}_{\alpha\gamma} + Q^{\mathrm{T}}_{\beta\gamma}\left(Q^{\mathrm{T}}_{\beta\beta} + Q^{\mathrm{T}}_{\gamma\gamma}\right)\right]$
$D^{\mathrm{Q},2}_{\frac{1}{2},\alpha}$	$-9\Lambda_{\mathrm{Q}}/8\left[\left(Q^{\mathrm{T}}_{\beta\beta} - Q^{\mathrm{T}}_{\gamma\gamma}\right)^2 - 4(Q^{\mathrm{T}}_{\beta\gamma})^2\right]$
$E^{\mathrm{Q},2}_{\frac{1}{2},\alpha}$	$9\Lambda_{\mathrm{Q}}/2Q^{\mathrm{T}}_{\beta\gamma}\left(Q^{\mathrm{T}}_{\gamma\gamma} - Q^{\mathrm{T}}_{\beta\beta}\right)$

where the subscripts x, y, and z refer to the rotation axes $-x^{\mathrm{T}}$, y^{T}, and $-z^{\mathrm{T}}$, respectively, and θ is the rotation angle (see section 2.1). Using these rotation matrices the resonance frequency for the first-order Hamiltonians becomes

$$\nu^{\lambda,1}_{m,\alpha}(\theta) = A^{\lambda,1}_{m,\alpha} + B^{\lambda,1}_{m,\alpha}\cos 2\theta + C^{\lambda,1}_{m,\alpha}\sin 2\theta \tag{3.28}$$

whereas the second-order quadrupolar term has two extra terms

$$\nu^{\mathrm{Q},2}_{m,\alpha}(\theta) = A^{\mathrm{Q},2}_{m,\alpha} + B^{\mathrm{Q},2}_{m,\alpha}\cos 2\theta + C^{\mathrm{Q},2}_{m,\alpha}\sin 2\theta + D^{\mathrm{Q},2}_{m,\alpha}\cos 4\theta + E^{\mathrm{Q},2}_{m,\alpha}\sin 4\theta. \tag{3.29}$$

The coefficients $M^{\lambda,n}_{m,\alpha}$ are given in table 3.3, expressed in terms of the $\lambda^{\mathrm{T}}_{\alpha\beta}$ tensor elements. The $M^{\mathrm{Q},2}_{m,\alpha}$ coefficients are only listed for the central ($1/2 \leftrightarrow -1/2$) transition.

3.2.2 The Two-Axis Goniometer

The T $\rightarrow$ L coordinate transformation for the geometry of our two-axis goniometer (section 2.2) is given by the rotation matrix

$$\mathbf{R}_\alpha(\theta) = \frac{1}{\sqrt{2}} \begin{pmatrix} \mu(\sin\phi + \cos\phi\cos\theta) & \mu\sin\theta & -\cos\phi + \sin\phi\sin\theta \\ -\mu\sqrt{2}\cos\phi\sin\theta & \mu\sqrt{2}\cos\theta & -\sqrt{2}\sin\phi\sin\theta \\ -\mu(\sin\phi - \cos\phi\cos\theta & \mu\sin\theta & \cos\phi + \sin\phi\cos\theta \end{pmatrix} \quad (3.30)$$

with $(\alpha, \mu) = (a, 1)$ or $(b, -1)$ and θ describing the rotation angle (see section 2.2). From this rotation matrix we can deduce the following resonance frequency for the first-order Hamiltonian

$$\nu_{m,\alpha}^{\lambda,1}(\theta) = A_{m,\alpha}^{\lambda,1} + B_{m,\alpha}^{\lambda,1}\cos\theta + C_{m,\alpha}^{\lambda,1}\sin\theta + D_{m,\alpha}^{\lambda,1}\cos 2\theta + E_{m,\alpha}^{\lambda,1}\sin 2\theta. \quad (3.31)$$

The main difference compared to the three-axis goniometer geometry is the two extra terms (proportional to $\cos\theta$ and $\sin\theta$) which are due to the 45° rotation axis of this goniometer. The equation for the second-order quadrupolar term is given by

$$\begin{aligned} \nu_{m,\alpha}^{\mathrm{Q},2}(\theta) \;=\; & A_{m,\alpha}^{\mathrm{Q},2} + B_{m,\alpha}^{\mathrm{Q},2}\cos\theta + C_{m,\alpha}^{\mathrm{Q},2}\sin\theta + D_{m,\alpha}^{\mathrm{Q},2}\cos 2\theta + E_{m,\alpha}^{\mathrm{Q},2}\sin 2\theta \\ & + F_{m,\alpha}^{\mathrm{Q},2}\cos 3\theta + G_{m,\alpha}^{\mathrm{Q},2}\sin 3\theta + H_{m,\alpha}^{\mathrm{Q},2}\cos 4\theta + I_{m,\alpha}^{\mathrm{Q},2}\sin 4\theta. \quad (3.32) \end{aligned}$$

The coefficients $M_{m,\alpha}^{\lambda,n}$ are given in table 3.4. The second-order quadrupolar coefficients, $M_{m,\alpha}^{\mathrm{Q},2}$ are only shown for the central $(1/2 \leftrightarrow -1/2)$ transition.

Table 3.4: Coefficients, $M^{\lambda,n}_{m,\alpha}$, for eqs. 3.31 and 3.32 expressed in terms of the $\lambda^{\mathrm{T}}_{\alpha\beta}$ tensor elements. The $M^{\mathrm{Q},2}_{m,\alpha}$ coefficients are only listed for the central transition ($m = 1/2$). The nomenclature used is $\Gamma_\sigma = -\nu_0$, $\Gamma_{\mathrm{Q}} = 3(m - 1/2)$, and for the central transition $\Lambda_{\mathrm{Q}} = (3 - 4I[I+1])/16\nu_0$. $(\alpha, \mu) = (a, 1)$, $(b, -1)$.

$A^{\lambda,1}_{m,\alpha}$	$\Gamma_\lambda/4 \left[\lambda^{\mathrm{T}}_{yy} + \left(\lambda^{\mathrm{T}}_{xx} + \lambda^{\mathrm{T}}_{zz}\right)\cos^2\phi - \mu 2\lambda^{\mathrm{T}}_{xz}\cos\phi\sin\phi + \left(2\lambda^{\mathrm{T}}_{xx} + \lambda^{\mathrm{T}}_{zz}\right)\sin^2\phi\right]$
$B^{\lambda,1}_{m,\alpha}$	$\Gamma_\lambda\mu/2 \left(\mu\lambda^{\mathrm{T}}_{xz}\cos^2\phi + \left(-\lambda^{\mathrm{T}}_{xx} + \lambda^{\mathrm{T}}_{zz}\right)\cos\phi\sin\phi - \mu\lambda^{\mathrm{T}}_{xz}\sin^2\phi\right)$
$C^{\lambda,1}_{m,\alpha}$	$\Gamma_\lambda \left(\mu\lambda^{\mathrm{T}}_{yz}\cos\phi - \lambda^{\mathrm{T}}_{xy}\sin\phi\right)$
$D^{\lambda,1}_{m,\alpha}$	$\frac{\Gamma_\lambda}{4} \left(-\lambda^{\mathrm{T}}_{yy} + \lambda^{\mathrm{T}}_{xx}\cos^2\phi + \mu 2\lambda^{\mathrm{T}}_{xz}\cos\phi\sin\phi + \lambda^{\mathrm{T}}_{zz}\sin^2\phi\right)$
$E^{\lambda,1}_{m,\alpha}$	$\frac{\Gamma_\lambda}{2} \left(\lambda^{\mathrm{T}}_{xy}\cos\phi + \mu\lambda^{\mathrm{T}}_{yz}\sin\phi\right)$
$A^{\mathrm{Q},2}_{\frac{1}{2},\alpha}$	$\frac{\Lambda_{\mathrm{Q}}}{512} \left(21(Q^{\mathrm{T}}_{yy})^2 + \left(28(Q^{\mathrm{T}}_{xy})^2 + 14Q^{\mathrm{T}}_{xx}Q^{\mathrm{T}}_{yy} + 16(Q^{\mathrm{T}}_{yz})^2 - 56Q^{\mathrm{T}}_{yy}Q^{\mathrm{T}}_{zz}\right)\cos^2\phi$ $+ \left(21(Q^{\mathrm{T}}_{xx})^2 + 16(Q^{\mathrm{T}}_{xz})^2 - 56Q^{\mathrm{T}}_{xx}Q^{\mathrm{T}}_{zz} + 56(Q^{\mathrm{T}}_{zz})^2\right)\cos^4\phi$ $+\mu 4 \left(35Q^{\mathrm{T}}_{xz}Q^{\mathrm{T}}_{yy} + 6Q^{\mathrm{T}}_{xy}Q^{\mathrm{T}}_{yz}\right)\cos\phi\sin\phi$ $+\mu 4Q^{\mathrm{T}}_{xz} \left(41Q^{\mathrm{T}}_{xx} - 76Q^{\mathrm{T}}_{zz}\right)\cos^3\phi\sin\phi$ $+2 \left(8(Q^{\mathrm{T}}_{xy})^2 - 28Q^{\mathrm{T}}_{xx}Q^{\mathrm{T}}_{yy} + 14(Q^{\mathrm{T}}_{yz})^2 + 7Q^{\mathrm{T}}_{yy}Q^{\mathrm{T}}_{zz}\right)\sin^2\phi$ $+2 \left(-20(Q^{\mathrm{T}}_{xx})^2 + 250(Q^{\mathrm{T}}_{xz})^2 + 61Q^{\mathrm{T}}_{xx}Q^{\mathrm{T}}_{zz} - 20(Q^{\mathrm{T}}_{zz})^2\right)\cos^2\phi\sin^2\phi$ $+\mu 4Q^{\mathrm{T}}_{xz} \left(-76Q^{\mathrm{T}}_{xx} + 41Q^{\mathrm{T}}_{zz}\right)\cos\phi\sin^3\phi$ $+ \left(56(Q^{\mathrm{T}}_{xx})^2 + 16(Q^{\mathrm{T}}_{xz})^2 - 56Q^{\mathrm{T}}_{xx}Q^{\mathrm{T}}_{zz} + 21(Q^{\mathrm{T}}_{zz})^2\right)\sin^4\phi\right)$
$B^{\mathrm{Q},2}_{\frac{1}{2},\alpha}$	$\frac{-\mu\Lambda_{\mathrm{Q}}}{64} \left(\left(17Q^{\mathrm{T}}_{xz}Q^{\mathrm{T}}_{yy} - 30Q^{\mathrm{T}}_{xy}Q^{\mathrm{T}}_{yz}\right)\cos^2\phi - Q^{\mathrm{T}}_{xz}\left(13Q^{\mathrm{T}}_{xx} + 4Q^{\mathrm{T}}_{zz}\right)\cos^4\phi\right.$ $+\mu \left(30(Q^{\mathrm{T}}_{xy})^2 - 17Q^{\mathrm{T}}_{xx}Q^{\mathrm{T}}_{yy} - 30(Q^{\mathrm{T}}_{yz})^2 + 17Q^{\mathrm{T}}_{yy}Q^{\mathrm{T}}_{zz}\right)\cos\phi\sin\phi$ $+\mu \left(13(Q^{\mathrm{T}}_{xx})^2 - 18(Q^{\mathrm{T}}_{xz})^2 - 9Q^{\mathrm{T}}_{xx}Q^{\mathrm{T}}_{zz} - 4(Q^{\mathrm{T}}_{zz})^2\right)\cos^3\phi\sin\phi$ $+ \left(-17Q^{\mathrm{T}}_{xz}Q^{\mathrm{T}}_{yy} + 30Q^{\mathrm{T}}_{xy}Q^{\mathrm{T}}_{yz}\right)\sin^2\phi + 27Q^{\mathrm{T}}_{xz}\left(Q^{\mathrm{T}}_{xx} - Q^{\mathrm{T}}_{zz}\right)\cos^2\phi\sin^2\phi$ $+\mu \left(4(Q^{\mathrm{T}}_{xx})^2 + 18(Q^{\mathrm{T}}_{xz})^2 + 9Q^{\mathrm{T}}_{xx}Q^{\mathrm{T}}_{zz} - 13\sec Q^{\mathrm{T}}_{zz}\right)\cos\phi\sin^3\phi$ $\left.+Q^{\mathrm{T}}_{xz}\left(4Q^{\mathrm{T}}_{xx} + 13Q^{\mathrm{T}}_{zz}\right)\sin^4\phi\right)$

contined on next page

Table 3.4 – continued from previous page

$C^{\mathrm{Q},2}_{\frac{1}{2},\alpha}$	$\frac{\Lambda_\mathrm{Q}}{64}\left(13Q^\mathrm{T}_{yy}Q^\mathrm{T}_{yz}\cos\phi+\left(30Q^\mathrm{T}_{xy}Q^\mathrm{T}_{xz}-17Q^\mathrm{T}_{xx}Q^\mathrm{T}_{yz}+4Q^\mathrm{T}_{yz}Q^\mathrm{T}_{zz}\right)\cos^3\phi\right.$ $-\mu 13Q^\mathrm{T}_{xy}Q^\mathrm{T}_{yy}\sin\phi+\mu\left(-13Q^\mathrm{T}_{xx}Q^\mathrm{T}_{xy}-12Q^\mathrm{T}_{xz}Q^\mathrm{T}_{yz}+26Q^\mathrm{T}_{xy}Q^\mathrm{T}_{zz}\right)\cos^2\phi\sin\phi$ $+\left(12Q^\mathrm{T}_{xy}Q^\mathrm{T}_{xz}-26Q^\mathrm{T}_{xx}Q^\mathrm{T}_{yz}+13Q^\mathrm{T}_{yz}Q^\mathrm{T}_{zz}\right)\cos\phi\sin^2\phi$ $\left.+\mu\left(-4Q^\mathrm{T}_{xx}Q^\mathrm{T}_{xy}-30Q^\mathrm{T}_{xz}Q^\mathrm{T}_{yz}+17Q^\mathrm{T}_{xy}Q^\mathrm{T}_{zz}\right)\sin^3\phi\right)$
$D^{\mathrm{Q},2}_{\frac{1}{2},\alpha}$	$\frac{-\Lambda_\mathrm{Q}}{128}\left(11(Q^\mathrm{T}_{yy})^2-2\left(6(Q^\mathrm{T}_{yz})^2+11Q^\mathrm{T}_{yy}Q^\mathrm{T}_{zz}\right)\cos^2\phi\right.$ $+\left(-11(Q^\mathrm{T}_{xx})^2+12(Q^\mathrm{T}_{xz})^2+22Q^\mathrm{T}_{xx}Q^\mathrm{T}_{zz}\right)\cos^4\phi$ $+\mu 4\left(11Q^\mathrm{T}_{xz}Q^\mathrm{T}_{yy}+6Q^\mathrm{T}_{xy}Q^\mathrm{T}_{yz}\right)\cos\phi\sin\phi$ $+\mu 4Q^\mathrm{T}_{xz}\left(-28Q^\mathrm{T}_{xx}+17Q^\mathrm{T}_{zz}\right)\cos^3\phi\sin\phi$ $-2\left(6(Q^\mathrm{T}_{xy})^2+11Q^\mathrm{T}_{xx}Q^\mathrm{T}_{yy}\right)\sin^2\phi$ $+2\left(17(Q^\mathrm{T}_{xx})^2-78(Q^\mathrm{T}_{xz})^2-23Q^\mathrm{T}_{xx}Q^\mathrm{T}_{zz}+17(Q^\mathrm{T}_{zz})^2\right)\cos^2\phi\sin^2\phi$ $+\mu 4Q^\mathrm{T}_{xz}\left(17Q^\mathrm{T}_{xx}-28Q^\mathrm{T}_{zz}\right)\cos\phi\sin^3\phi$ $\left.+\left(12(Q^\mathrm{T}_{xz})^2+22Q^\mathrm{T}_{xx}Q^\mathrm{T}_{zz}-11(Q^\mathrm{T}_{zz})^2\right)\sin^4\phi\right)$
$E^{\mathrm{Q},2}_{\frac{1}{2},\alpha}$	$\frac{\Lambda_\mathrm{Q}}{64}\left(11Q^\mathrm{T}_{xy}Q^\mathrm{T}_{yy}\cos\phi+\left(11Q^\mathrm{T}_{xx}Q^\mathrm{T}_{xy}-12Q^\mathrm{T}_{xz}Q^\mathrm{T}_{yz}-22Q^\mathrm{T}_{xy}Q^\mathrm{T}_{zz}\right)\cos^3\phi\right.$ $+\mu 11Q^\mathrm{T}_{yy}Q^\mathrm{T}_{yz}\sin\phi+\mu\left(78Q^\mathrm{T}_{xy}Q^\mathrm{T}_{xz}+23Q^\mathrm{T}_{xx}Q^\mathrm{T}_{yz}-34Q^\mathrm{T}_{yz}Q^\mathrm{T}_{zz}\right)\cos^2\phi\sin\phi$ $+\left(-34Q^\mathrm{T}_{xx}Q^\mathrm{T}_{xy}+78Q^\mathrm{T}_{xz}Q^\mathrm{T}_{yz}+23Q^\mathrm{T}_{xy}Q^\mathrm{T}_{zz}\right)\cos\phi\sin^2\phi$ $\left.+\mu\left(-12Q^\mathrm{T}_{xy}Q^\mathrm{T}_{xz}-22Q^\mathrm{T}_{xx}Q^\mathrm{T}_{yz}+11Q^\mathrm{T}_{yz}Q^\mathrm{T}_{zz}\right)\sin^3\phi\right)$
$F^{\mathrm{Q},2}_{\frac{1}{2},\alpha}$	$\frac{9\Lambda_\mathrm{Q}}{64}\left(-\left(Q^\mathrm{T}_{xz}Q^\mathrm{T}_{yy}+2Q^\mathrm{T}_{xy}Q^\mathrm{T}_{yz}\right)\cos^2\phi+Q^\mathrm{T}_{xx}Q^\mathrm{T}_{xz}\cos^4\phi\right.$ $+\mu\left(2(Q^\mathrm{T}_{xy})^2+Q^\mathrm{T}_{xx}Q^\mathrm{T}_{yy}-2(Q^\mathrm{T}_{yz})^2-Q^\mathrm{T}_{yy}Q^\mathrm{T}_{zz}\right)\cos\phi\sin\phi$ $+\mu\left(-(Q^\mathrm{T}_{xx})^2+2(Q^\mathrm{T}_{xz})^2+Q^\mathrm{T}_{xx}Q^\mathrm{T}_{zz}\right)\cos^3\phi\sin\phi$ $+\left(Q^\mathrm{T}_{xz}Q^\mathrm{T}_{yy}+2Q^\mathrm{T}_{xy}Q^\mathrm{T}_{yz}\right)\sin^2\phi-3Q^\mathrm{T}_{xz}\left(Q^\mathrm{T}_{xx}-Q^\mathrm{T}_{zz}\right)\cos^2\phi\sin^2\phi$ $\left.-\mu\left(2(Q^\mathrm{T}_{xz})^2+Q^\mathrm{T}_{xx}Q^\mathrm{T}_{zz}-(Q^\mathrm{T}_{zz})^2\right)\cos\phi\sin^3\phi-Q^\mathrm{T}_{xz}Q^\mathrm{T}_{zz}\sin^4\phi\right)$

contined on next page

Table 3.4 – continued from previous page

$G^{\mathrm{Q},2}_{\frac{1}{2},\alpha}$	$\frac{\mu 9\Lambda_{\mathrm{Q}}}{64}\Big(Q^{\mathrm{T}}_{yy}Q^{\mathrm{T}}_{yz}\cos\phi-\Big(2Q^{\mathrm{T}}_{xy}Q^{\mathrm{T}}_{xz}+Q^{\mathrm{T}}_{xx}Q^{\mathrm{T}}_{yz}\Big)\cos^3\phi-\mu Q^{\mathrm{T}}_{xy}Q^{\mathrm{T}}_{yy}\sin\phi$ $+\mu\Big(3Q^{\mathrm{T}}_{xx}Q^{\mathrm{T}}_{xy}-4Q^{\mathrm{T}}_{xz}Q^{\mathrm{T}}_{yz}-2Q^{\mathrm{T}}_{xy}Q^{\mathrm{T}}_{zz}\Big)\cos^2\phi\sin\phi$ $+\Big(4Q^{\mathrm{T}}_{xy}Q^{\mathrm{T}}_{xz}+2Q^{\mathrm{T}}_{xx}Q^{\mathrm{T}}_{yz}-3Q^{\mathrm{T}}_{yz}Q^{\mathrm{T}}_{zz}\Big)\cos\phi\sin^2\phi$ $+\mu\Big(2Q^{\mathrm{T}}_{xz}Q^{\mathrm{T}}_{yz}+Q^{\mathrm{T}}_{xy}Q^{\mathrm{T}}_{zz}\Big)\sin^3\phi\Big)$
$H^{\mathrm{Q},2}_{\frac{1}{2},\alpha}$	$\frac{-9\Lambda_{\mathrm{Q}}}{512}\Big((Q^{\mathrm{T}}_{yy})^2-2\Big(2(Q^{\mathrm{T}}_{xy})^2+Q^{\mathrm{T}}_{xx}Q^{\mathrm{T}}_{yy}\Big)\cos^2\phi+(Q^{\mathrm{T}}_{xx})^2\cos^4\phi$ $-\mu 4\Big(Q^{\mathrm{T}}_{xz}Q^{\mathrm{T}}_{yy}+2Q^{\mathrm{T}}_{xy}Q^{\mathrm{T}}_{yz}\Big)\cos\phi\sin\phi+\mu 4Q^{\mathrm{T}}_{xx}Q^{\mathrm{T}}_{xz}\cos^3\phi\sin\phi$ $-2\Big(2(Q^{\mathrm{T}}_{yz})^2+Q^{\mathrm{T}}_{yy}Q^{\mathrm{T}}_{zz}\Big)\sin^2\phi+2\Big(2(Q^{\mathrm{T}}_{xz})^2+Q^{\mathrm{T}}_{xx}Q^{\mathrm{T}}_{zz}\Big)\cos^2\phi\sin^2\phi$ $+\mu 4Q^{\mathrm{T}}_{xz}Q^{\mathrm{T}}_{zz}\cos\phi\sin^3\phi+4(Q^{\mathrm{T}}_{zz})^2\sin^4\phi\Big)$
$I^{\mathrm{Q},2}_{\frac{1}{2},\alpha}$	$\frac{9\Lambda_{\mathrm{Q}}}{128}\Big(\Big(Q^{\mathrm{T}}_{xy}\cos\phi+\mu Q^{\mathrm{T}}_{yz}\sin\phi\Big)$ $\times\Big(Q^{\mathrm{T}}_{yy}-Q^{\mathrm{T}}_{xx}\cos^2\phi-\mu 2Q^{\mathrm{T}}_{xz}\cos\phi\sin\phi-Q^{\mathrm{T}}_{zz}\sin^2\phi\Big)\Big)$

3.3 Simulation of Spectra for Polycrystalline Samples

The main difference between simulation of NMR spectra of single crystals and polycrystalline samples is the need for a powder averaging when simulating powder NMR spectra. A typical polycrystalline sample contains in the order of 10^8 different crystallites (*81*), but summation of that many subspectra (one spectrum for each crystallite) would be very time-consuming. Thus, the need for efficient powder averaging schemes is obvious and has been adressed by several groups (*44*, *81–90*). Some averaging schemes allow interpolation between the different crystallites (*85*), a feature that reduces the number of crystallites to $\approx$ 1000 for simulation of a second-order quadrupolar lineshape.

Because of the requirement for orientational averaging it is beneficial to express the Hamiltonian in the irreducible tensor formalism (eqs. 3.13 - 3.15) as the coordinate transformations require fewer operations in this basis than in the cartesian

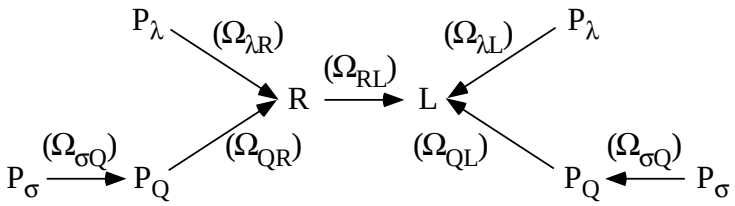

Figure 3.3: Coordinate transformations used for simulation of powder spectra. For a static sample influenced by one interaction only the coordinate transformation from P_λ to L is needed. If sample spinning is applied we need to introduce the rotor frame (R).

representation. The λ_{00} element is invariant to coordinate transformations, while the $\lambda^{\mathrm{L}}_{2m}$ elements are calculated via the series of coordinate transformations given in fig. 3.3. The coordinate transformations starting from left apply to MAS spectra where a rotor frame (R) is introduced, while this coordinate system is omitted for simulation of static spectra. Similarly to the simulation of SC NMR spectra I will use the route $P_\sigma \rightarrow P_Q(\rightarrow R) \rightarrow L$ when the combined effect of CSA and quadrupole coupling is present. In the following I shall only discuss simulations of spectra of the central transition for half-integer quadrupolar nuclei influenced by the combined effect of quadrupole coupling and CSA.

3.3.1 Static Powder

The spectrum ($\mathcal{S}(\omega)$) for a static powder is given by a sum of SC spectra for all crystallite orientations (Ω_{QL})

$$\mathcal{S}(\omega) = \sum_{\Omega_{\mathrm{QL}}} \mathcal{S}(\Omega_{\mathrm{QL}};\omega), \tag{3.33}$$

and the spectrum for each crystallite is a delta function, $\mathcal{S}(\Omega_{\mathrm{QL}};\omega) = \delta_{\omega,\omega(\Omega_{\mathrm{QL}})} W(\Omega_{\mathrm{QL}})$ with its peak located at the resonance frequency

$$\begin{aligned}\omega(\Omega_{\mathrm{QL}}) &= \frac{1}{2\omega_0}\left(1/2 Q^{\mathrm{L}}_{2-2}(\Omega_{\mathrm{QL}}) Q^{\mathrm{L}}_{22}(\Omega_{\mathrm{QL}}) + Q^{\mathrm{L}}_{2-1}(\Omega_{\mathrm{QL}}) Q^{\mathrm{L}}_{21}(\Omega_{\mathrm{QL}})\right)[4I(I+1)-3] \\ &\quad + \frac{\omega_0}{\sqrt{3}}\left(-\sigma_{00} + \sqrt{2}\sigma^{\mathrm{L}}_{20}(\Omega_{\mathrm{QL}})\right)\end{aligned} \tag{3.34}$$

and with a weight $W(\Omega_{\mathrm{QL}})$ that corresponds to the solid angle of the particular crystallite. The elements of the quadrupole coupling tensor are given by

$$Q^{\mathrm{L}}_{2m}(\Omega_{\mathrm{QL}}) = \frac{2\pi C_{\mathrm{Q}}}{2I(2I-1)}\left(\mathfrak{D}^{(2)}_{0m}(\Omega_{\mathrm{QL}}) - \frac{\eta_{\mathrm{Q}}}{2}\left(\mathfrak{D}^{(2)}_{2m}(\Omega_{\mathrm{QL}}) + \mathfrak{D}^{(2)}_{-2m}(\Omega_{\mathrm{QL}})\right)\right) \quad (3.35)$$

and the second-rank CSA element is ($\sigma^{\mathrm{L}}_{00} \equiv \sigma^{\mathrm{P}_\sigma}_{00}$)

$$\begin{aligned}\sigma^{\mathrm{L}}_{20}(\Omega_{\mathrm{QL}}) &= \omega_0\delta_\sigma \times \\ &\sum_{m=-2}^{2}\left(\mathfrak{D}^{(2)}_{0m}(\psi,\chi,\xi) - \frac{\eta_\sigma}{2}\left(\mathfrak{D}^{(2)}_{2m}(\psi,\chi,\xi) + \mathfrak{D}^{(2)}_{-2m}(\psi,\chi,\xi)\right)\right)\mathfrak{D}^{(2)}_{m0}(\Omega_{\mathrm{QL}}). \quad (3.36)\end{aligned}$$

It is noted that we only need a summation over two of the Euler angles, $\Omega_{\mathrm{QL}} = (\alpha_{\mathrm{Q}}, \beta_{\mathrm{Q}}, 0)$, for the powder averaging, because the angle γ_{Q} only represents a rotation about the B_0 field.

3.3.2 Magic-Angle Spinning

When MAS is applied, the simulation becomes slightly more complicated because the sample rotation introduces a time dependence of the $\lambda^{\mathrm{L}}_{2m}$ terms of the Hamiltonian (periodic with the rotor-period $\tau_{\mathrm{r}} = 1/\nu_{\mathrm{r}}$).[8] The Euler angles describing the R $\rightarrow$ L transformation are given by $\Omega_{\mathrm{RL}} = (\omega_{\mathrm{r}}t, \Theta, 0)$ where Θ is the magic angle ($\Theta = \tan^{-1}\sqrt{2}$). The quadrupole coupling and CSA elements $\lambda^{\mathrm{L}}_{2m}$ are given by

$$\begin{aligned}Q^{\mathrm{L}}_{2m}(\Omega_{\mathrm{QL}};t) &= \frac{2\pi C_{\mathrm{Q}}}{2I(2I-1)}\sum_{m'=-2}^{2}\exp(-im'\omega_{\mathrm{r}}t)d^{(2)}_{m'm}(\Theta)\times\left(\mathfrak{D}^{(2)}_{0m'}(\Omega_{\mathrm{QR}})\right. \\ &\left. -\frac{\eta_{\mathrm{Q}}}{2}\left[\mathfrak{D}^{(2)}_{2m'}(\Omega_{\mathrm{QR}}) + \mathfrak{D}^{(2)}_{2-m'}(\Omega_{\mathrm{QR}})\right]\right) \quad (3.37)\end{aligned}$$

[8] The tensor elements $\lambda^{\mathrm{L}}_{2m}$ have been assumed time-independent in integration that leads to the average Hamiltonian (eqs. 3.12 - 3.15). However, the $\lambda^{\mathrm{L}}_{2m}$ elements are approximately constant on the timescale of the averaging (τ_0) which is several orders of magnitude smaller than the rotor period.

and

$$\sigma_{20}^{\mathrm{L}}(\Omega_{\mathrm{QL}};t) = \omega_0\delta_\sigma \sum_{m'=-2}^{2} \left\{ \left(\mathfrak{D}^{(2)}_{0m'}(\psi,\chi,\xi) - \frac{\eta_\sigma}{2}\left[\mathfrak{D}^{(2)}_{2m'}(\psi,\chi,\xi) + \mathfrak{D}^{(2)}_{-2m'}(\psi,\chi,\xi)\right]\right) \times \mathfrak{D}^{(2)}_{m'm}(\Omega_{\mathrm{QR}}) \exp(-im'\omega_{\mathrm{r}}t) d^{(2)}_{m'0}(\Theta) \right\}. \quad (3.38)$$

These equations use a decomposition of the Wigner elements $\mathfrak{D}^{(2)}_{m'm}(\alpha,\beta,\gamma)$ into reduced Wigner elements ($d^{(2)}_{m'm}$) according to $\mathfrak{D}^{(2)}_{m'm} = e^{-im'\alpha} d^{(2)}_{m'm}(\beta) e^{-im\gamma}$ (*76*). It should be pointed out that the powder averaging of MAS NMR spectra requires summation of all three powder Euler angles.

The simulation of MAS NMR spectra is further complicated as the resonance frequency of each crystallite varies in time. Thus we need to calculate the signal in time-domain ($s(\Omega_{\mathrm{QR}};\omega_{\mathrm{r}}t)$). Using quadrature detection the signal $s(t)$ is given as the projection of the density operator $\tilde{\rho}$ onto the I_- operator:

$$\begin{aligned} \mathcal{S}(\Omega_{\mathrm{QR}};\omega_{\mathrm{r}}t) &= \langle I_-|\tilde{\rho}(\Omega_{\mathrm{QR}};\omega_{\mathrm{r}}t)\rangle = \mathrm{Tr}\{\tilde{\rho}(\Omega_{\mathrm{QR}};\omega_{\mathrm{r}}t) I_+\} \\ &= \sum_{m,n=-I}^{I} \langle m|\tilde{\rho}(\Omega_{\mathrm{QR}};\omega_{\mathrm{r}}t)|n\rangle\langle n|I_+|m\rangle = \tilde{\rho}_{m-1,m}(\Omega_{\mathrm{QR}};\omega_{\mathrm{r}}t)\sqrt{p_m} \quad (3.39) \end{aligned}$$

where $p_m = I(I+1) - m(m-1)$ is the transition probability for the $m \leftrightarrow m-1$ transition. The evolution of the density operator is given by the Liouville von Neuman equation (see footnote 5 on page 30) as

$$\tilde{\rho}(\Omega_{\mathrm{QR}};\omega_{\mathrm{r}}t) = \tilde{U}(\Omega_{\mathrm{QR}};\omega_{\mathrm{r}}t)\tilde{\rho}(\Omega_{\mathrm{QR}};0)\tilde{U}^{\dagger}(\Omega_{\mathrm{QR}};\omega_{\mathrm{r}}t), \quad (3.40)$$

$$\tilde{U}(\Omega_{\mathrm{QR}};\omega_{\mathrm{r}}t) = T\exp\left\{-i\int_0^t \overline{\widetilde{\mathcal{H}}}(\Omega_{\mathrm{QR}};\omega_{\mathrm{r}}t')dt'\right\}. \quad (3.41)$$

T is the Dyson time-ordering operator (*91*) that ensures a chronologic evaluation of the integral in the case of a homogeneous Hamiltonian. In the secular approximation both the CSA and first- and second-order quadrupolar interactions are inhomogeneous, and thus we may disregard the Dyson operator. The density operator may

be calculated in the Zeeman base ($|m\rangle$) according to

$$\begin{aligned}\widetilde{\rho}_{m-1,m}(\Omega_{\mathrm{QR}};\omega_{\mathrm{r}}t) &= \sum_{n,n'}\overline{c_n(0)c^*_{n'}(0)}\langle m-1|\widetilde{U}(\Omega_{\mathrm{QR}};\omega_{\mathrm{r}}t)|n\rangle\langle n'|\widetilde{U}^{-1}(\Omega_{\mathrm{QR}};\omega_{\mathrm{r}}t)|m\rangle \\ &= \widetilde{\rho}_{m-1,m}(\Omega_{\mathrm{QR}};0)\exp\left\{i\int_0^t\omega_m(\Omega_{\mathrm{QR}};\omega_{\mathrm{r}}t')dt'\right\}, \qquad (3.42)\end{aligned}$$

where the time-dependent "resonance frequency" (ω_m) is similar to that in eq. 3.34. The initial density operator $\widetilde{\rho}(\Omega_{\mathrm{QR}};0^-)$ corresponds to thermal equilibrium $\widetilde{\rho}(\Omega_{\mathrm{QR}};0^-) = \widetilde{\rho}_{\mathrm{eq}} = I_z$, and if this magnetization is excited by an ideal 90°_x-pulse we obtain the density operator $\widetilde{\rho}(\Omega_{\mathrm{QR}};0^+) = -I_y$ or more convenient $\widetilde{\rho}_{m-1,m}(\Omega_{\mathrm{QR}};0^+) = \langle m-1|I_-|m\rangle = \sqrt{p_m}$. Thus, the signal (FID) is given by

$$\mathcal{S}_m(\alpha_{\mathrm{Q}},\beta_{\mathrm{Q}},\gamma_{\mathrm{Q}};\omega_{\mathrm{r}}t) = p_m\exp\{i\Phi_m(\alpha_{\mathrm{Q}},\beta_{\mathrm{Q}},\gamma_{\mathrm{Q}};\omega_{\mathrm{r}}t)\} \qquad (3.43)$$

with the "phase"

$$\Phi_m(\alpha_{\mathrm{Q}},\beta_{\mathrm{Q}},\gamma_{\mathrm{Q}};\omega_{\mathrm{r}}t) = \int_0^t\omega_m(\alpha_{\mathrm{Q}},\beta_{\mathrm{Q}},\gamma_{\mathrm{Q}};\omega_{\mathrm{r}}t')dt' \qquad (3.44)$$

from which the FID may be calculated.

It is noted that the angles γ_{Q} and $\omega_{\mathrm{r}}t$ always enter eq. 3.44 as $\omega_{\mathrm{r}}t+\gamma_{\mathrm{Q}}$. Thus, if we disregard the constant terms (in time) of eq. 3.44 we obtain the relation[9]

$$\Phi_m(\alpha_{\mathrm{Q}},\beta_{\mathrm{Q}},\gamma_{\mathrm{Q}};\omega_{\mathrm{r}}t) = \Phi_m(\alpha_{\mathrm{Q}},\beta_{\mathrm{Q}},0;\omega_{\mathrm{r}}t+\gamma_{\mathrm{Q}}) - \Phi_m(\alpha_{\mathrm{Q}},\beta_{\mathrm{Q}},0;\gamma_{\mathrm{Q}}) \qquad (3.45)$$

which allows us to do the incrementation in time and averaging of γ_{Q} simultaneously with the fourier-transformation that takes the form of an auto-correlation (*74*, *92*). Thereby, the remaining averaging of the Euler angles α_{Q} and β_{Q} may be performed in the frequency domain which gives the possibility for interpolation in the powder averaging.

[9] Equation 3.44 only has constant terms for the second-order quadrupolar interaction. In fact, it is the constant terms that give the second-order lineshape in MAS spectra of quadrupolar nuclei.